ORIGINAL PAPER

Food Quality Evaluation using Model Foods: a Comparison Study between Microwave-Assisted and Conventional Thermal Pasteurization Processes

Ellen R. Bornhorst[1] · Fang Liu[1] · Juming Tang[1] · Shyam S. Sablani[1] ·
Gustavo V. Barbosa-Cánovas[1]

Abstract Thermal process optimization has focused on traditional sterilization, with limited research on pasteurization or microwave-assisted thermal processing. Model foods have been developed as quality evaluation tools for thermal pasteurization processes, but there are no comprehensive studies demonstrating how these model foods could be used to evaluate and compare the resulting food quality after different pasteurization processes. The aim of this study was to develop a methodology using image and quantitative analyses for quality evaluation of pre-packaged food pasteurized using a microwave-assisted pasteurization system (MAPS) and traditional hot water method. Four pasteurization processes (MAPS and hot water method at 90 and 95 °C) were designed to have an equivalent accumulated thermal lethality at the cold spot of at least 90 °C for 10 min to control nonproteolytic *Clostridium botulinum* spores. Color-based time-temperature indicators in mashed potato and green pea model foods were quantified using image analysis. Results showed that median color values were useful in assessing overall color change, and interquartile range was an indicator of burnt areas. MAPS 95 °C was the best process because it had the smallest hot spot cook values and the least color change, while the 90 °C hot water process was the worst. Model foods and image analysis techniques were useful pasteurization process quality evaluation tools and made it possible to visualize the potential food quality change volumetrically, throughout a food package. In the future, these tools could be combined with computer simulations to optimize the quality of pilot-scale and industrial MAPS or conventional pasteurization processes.

Keywords Food quality · Color change · Mashed potato · Green pea · Pasteurization

Introduction

The purpose of thermal pasteurization is to preserve food by eliminating pathogenic microorganisms and reducing the overall microbial load. In general, pasteurized products require a less severe heat treatment and have a better quality compared to commercially sterile products that have been thermally sterilized (retort or canned products). However, pasteurized products require chilled storage because the less severe thermal process does not inactivate proteolytic *Clostridium botulinum* spores; refrigeration can prevent their growth (Peck 2006). Guidelines for pasteurization processes for chilled food focus on achieving at least 6 log reductions of target pathogens. For example, to control nonproteolytic *C. botulinum* spores, an equivalent heat treatment of 90 °C for 10 min is recommended, whereas to control *Listeria monocytogenes*, 70 °C for 2 min is recommended (FDA 2011; ECFF 2006). These differing thermal severities yield products with varying shelf lives; the recommended maximum shelf life at ≤5 °C is ≤10 days for a product with a 70 °C for 2 min heat treatment and ≤6 weeks for a product with a 90 °C for 10-min heat treatment (Peck 2006; ECFF 2006; CSIRO 2010; Peng et al. 2015). In this study, the target thermal treatment was a 90 °C for 10 min process to control nonproteolytic *C. botulinum* spores.

Two pasteurization processes were examined in this study: a microwave-assisted pasteurization system (MAPS) and a

✉ Juming Tang
jtang@wsu.edu

1 Department of Biological Systems Engineering, Washington State University, L.J. Smith 204, P.O. Box 64120, Pullman, WA 99164-6120, USA

conventional hot water heating treatment. The MAPS was developed at Washington State University to leverage the rapid heating of microwaves (915 MHz) and shorten the come-up time for the product temperature to reach the target temperature (Tang 2015). By shortening the come-up time, the product quality can be improved compared to conventional hot water heating (Tang 2015).

The goal of optimizing thermal processes is to improve the overall food quality, with the constraint that the food product must be adequately heated at the coldest spot to be considered safe. Theoretically, high-temperature, short-time processes can produce higher quality products that are still safe (Holdsworth 1997). Previous work on thermal process optimization has focused on thermal sterilization for canning applications, using both a theoretical approach (e.g., mathematical model, finite element analysis) (Miri et al. 2008; Hildenbrand 1980; Teixeira et al. 1969) and experimental approach (e.g., measurement of thiamin or color retention) (Smout et al. 2003; Avila et al. 1999; Teixeira et al. 1975; Singh and Ramaswamy 2015). More recent research has focused on thermal pasteurization quality optimization for pre-packaged foods (Renna et al. 2013; Lespinard et al. 2015; Benlloch-Tinoco et al. 2014; Chakraborty et al. 2015; Marszalek et al. 2016).

Typical optimization of traditional thermal processes combines pathogen and quality degradation kinetics with predictable heating patterns generated from reliable mathematical models and computer simulations (Holdsworth 1997). However, optimization of newer thermal processing technologies, such as microwave heating, is more challenging because it requires more sophisticated mathematical models and computer simulations with more complicated heating patterns that can be difficult to validate (Tang 2015; Datta 2008). This type of complex simulation and numerical modeling for microwave heating systems was not even possible until the late 1980s; now calculation intensive models are possible because of advances in computer technology and increased computing power (Datta and Anantheswaran 2001; Chandrasekaran et al. 2013). However, the high degree of model complexity required to accurately simulate microwave heating systems results in models that can predict heating patterns but are not currently sophisticated enough to incorporate mathematical optimizations (Resurreccion et al. 2013; Chen et al. 2008; Pathak et al. 2003; Cha-um et al. 2011; Tang 2015). In order to optimize microwave-assisted thermal processes, new tools are needed to help assess and visualize product quality and validate predicted heating patterns and temperature profiles generated by computer simulations. Therefore, the focus of this research was to develop a methodology based on image and quantitative analyses for quality evaluation of pre-packaged, pasteurized food, especially food pasteurized using MAPS.

Mashed potato and green pea model foods have been developed as quality evaluation tools for use in process development and optimization of MAPS or traditional

pasteurization methods (Bornhorst et al. 2017a, b, c). Previous work focused on model food development and reaction kinetic determination. An initial model validation was conducted using MAPS and hot water pasteurization methods for a mashed potato model food by Bornhorst et al. (2017b) and a green pea model food by Bornhorst et al. (2017c). However, a comprehensive study demonstrating how these model foods could be used to evaluate and compare the quality of different pasteurization processes is needed. The objectives of this study were to (1) develop four pasteurization process schedules for pre-packaged trays of mashed potato and green pea model foods using MAPS and traditional hot water processes at 90 and 95 °C and (2) evaluate the color change and potential food quality of the pasteurized model foods.

Materials and Methods

Model Food Preparation

Mashed potato and green pea model foods were selected for analysis in this study. Previous work (Bornhorst et al. 2017b, c) on model food development for pasteurization applications indicated that color change in green pea puree model food and mashed potato with 1% added ribose and lysine would be ideal for evaluating food quality in processes targeting a 90 °C for 10-min thermal treatment. Two model foods were selected for analysis because the temperature sensitivity differed in each model food. The mashed potato model food color change had a z-value of 20.8 °C (L* value) and 25.6 °C (a* value) (Bornhorst et al. 2017b), compared to a z-value of 39.9 °C (a* value) for the green pea model food (Bornhorst et al. 2017c). By using both model foods, a larger range of food quality attributes' temperature sensitivity was covered (z-value 20–40 °C). Both model foods included 0.5% added sodium chloride (NaCl) to more closely resemble the dielectric properties of relevant food products that would be pre-packaged and pasteurized.

Preparation methods for the mashed potato model from Bornhorst et al. (2017a) were designed for small batches in bench-top reaction kinetic experiments. These methods were scaled-up and modified to be feasible for larger batch sizes required for this case study and future applications in evaluating pilot-scale and industrial processes. The mashed potato model food in this study consisted of 15% instant mashed potato flakes (Oregon Potato Co., Boardman, OR, USA), 0.75% low acyl gellan gum (Kelcogel® F Food grade gellan gum, supplied by CP Kelco Inc., Atlanta, GA, USA), 0.20% calcium chloride ($CaCl_2 \cdot 2H_2O$, J.T. Baker, Avantor Performance Materials, Inc., Center Valley, PA, USA), 0.5% anhydrous sodium chloride (J.T. Baker, Phillipsburg, NJ, USA), 1% D-ribose (Sigma-Aldrich Co. LLC, St. Louis,

MO, USA), 1% L-lysine (Sigma-Aldrich Co. LLC, St. Louis, MO, USA), and 81.55% deionized and distilled (DDI) water (Bornhorst et al. 2017a). The DDI water was heated to boiling in an electric kettle (Hamilton Beach, Richmond, VA, USA) and poured into a Vitamix blender (Vitamix 7500 machine, Vitamix Corp., Cleveland, OH, USA). The water was heated for an additional 2 min using the Vitamix blender until the temperature reached 95 °C, at which point salt and gellan gum were mixed in for 30 s. The potato flakes were mixed in for 1 min, followed by the addition of calcium chloride, which was mixed in for 1 min (solution temperature 90 °C). After cooling the solution to 60 °C, the ribose and lysine were mixed in for 1 min to achieve a uniform solution. Two hundred eighty grams of the model food was filled into a rectangular, rigid, polypropylene tray (116-mm width, 161-mm length, 32-mm depth) sealed with plastic lid-stock (Printpack, Inc., Atlanta, GA, USA) under 15 MPa of vacuum using a Multivac T200 tray sealer (Multivac, Wolfertschwenden, Germany).

The green pea model food consisted of 98.5% thawed, frozen green peas (Better Living Brands LLC, Pleasanton, CA, USA), 1% low acyl gellan gum, and 0.5% anhydrous sodium chloride (Bornhorst et al. 2017c). Procedures to prepare the green pea model food were adapted from Bornhorst et al. (2017c) as follows: frozen peas were thawed in warm water (40 °C), pureed in a Vitamix blender, and salt and gellan gum were thoroughly mixed into the pea puree. The green pea model food was also sealed under vacuum in polypropylene trays (280 g per tray), as described above.

Thermal Pasteurization

Trays of model foods were pasteurized using two target hot water temperatures (90 and 95 °C) in two different systems: a MAPS and a conventional hot water method. As described in Tang (2015), the MAPS process design has no overpressure and uses a warm water preheating step (30 min in 60 °C water), followed by exposure to single-mode 915 MHz microwaves in recirculating hot water (1.7 min at 90 or 95 °C water), holding in recirculating hot water (90 or 95 °C), and cooling in 23 °C water. The hot water method utilized a recirculating hot water bath (90 or 95 °C) with no overpressure (HAAKE DC 30, Thermo Fisher Scientific Inc., Newington, NH, USA), followed by cooling in 3 °C water.

Preliminary MAPS runs were performed to determine the cold spot and hot spot locations in trays of model foods. Compared to the center of the tray, the cold spot was 26 mm to the right and 12 mm below the center and the hot spot was 14 mm to the left and 38 mm above the center for the MAPS process (Fig. 1). For the hot water process, the cold spot was at the geometric center and the hot spot was at the corner of the tray (Fig. 1). The temperature at the cold spots were measured to ensure the process schedule produced a safely pasteurized food, while the temperature at the hot spots were measured to give an indication of quality and the temperature history of overheated or burnt areas. These temperatures were measured in 2 s intervals with calibrated mobile metallic sensors and data logging software (TMI-USA, Inc., Reston, VA, USA) (Luan et al. 2013).

Process development was performed for each MAPS and hot water process using several iterations and changing heating and holding times to determine a process schedule with adequate heat treatment at the cold spot. All the processes were designed to have an equivalent accumulated thermal lethality of at least 90 °C for 10 min at the cold spot to control nonproteolytic *C. botulinum* spores (FDA 2011; ECFF 2006). For the target pathogen (nonproteolytic *C. botulinum* spores), accumulated thermal lethality was calculated at the cold and

Fig. 1 Locations of the cold and hot spots in the middle layer of model foods pasteurized with the microwave-assisted pasteurization system (MAPS) (**a**) and hot water (**b**) processes. Coordinates of each location (*x*,*y*) are shown as the distance (mm) from the geometric center of the tray (0,0) (color figure online)
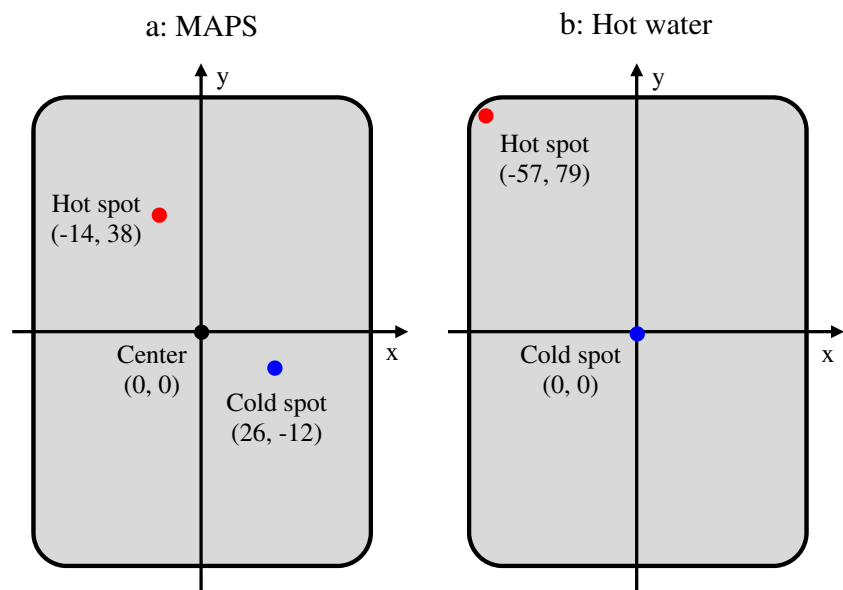
hot spots using the measured time-temperature histories with (Holdsworth 1997):

$$F_{90} = \int_0^t 10^{(T-90)/z} dt \qquad (1)$$

where F_{90} is the equivalent thermal treatment time (min) at 90 °C, T is the temperature (°C) at time t (min), and z is the thermal resistance constant (10 °C for this target pathogen) (FDA 2011; ECFF 2006). A commonly used indicator of food quality is the accumulated cook value or C_{100}, which was determined at the cold and hot spots using the measured time-temperature histories with (Holdsworth 1997):

$$C_{100} = \int_0^t 10^{(T-100)/z} dt \qquad (2)$$

where C_{100} is the equivalent thermal treatment time (min) at 100 °C, T is the temperature (°C) at time t (min), and z is the thermal resistance constant (°C). For the mashed potato model food, a z-value of 23 °C was utilized in the C_{100} calculation based on the average z-values for L* (20.8 °C) and a* (25.6 °C) reported by Bornhorst et al. (2017b). For the green pea model food, a z-value of 40 °C was utilized in the C_{100} calculation based on the a* z-value (39.9 °C) reported by Bornhorst et al. (2017c).

After the process schedules were determined for all four processes (MAPS at 90 and 95 °C and hot water at 90 and 95 °C), eight trays of both mashed potato and green pea model foods were pasteurized to assess the potential food quality of each process. The MAPS design is a pilot-scale system where four trays are typically processed in one run, while the hot water method utilized a smaller setup with one run consisting of two trays. For each temperature, two independent runs of four trays each were utilized to pasteurize the model foods with the MAPS and four independent runs of two trays each utilized to pasteurize the model foods with the hot water method.

Data Analysis

Color was quantified using the L*a*b* (CIELAB) color space commonly used for food applications, where L* represents lightness (black to white), a* represents green to red, and b* represents blue to yellow (Leon et al. 2006). Color in each tray of model food was assessed in four different layers: top layer (model food touching the plastic lid-stock film), middle layer (one half the sample thickness measured from the bottom), quarter layer (one fourth the sample thickness measured from the bottom), and bottom layer (model food touching the bottom of the rigid tray).

The color of each layer and unheated, control samples were analyzed by a computer vision system described in Bornhorst et al. (2017a). Briefly, the components included a digital camera (settings 1/15 s, ISO 200, F 11) connected to a computer with image acquisition software, light pod, compact fluorescent light bulbs, and image analysis. MATLAB R2013a was used for image analysis, which included color correction and

conversion from RGB to L*a*b*(CIELAB) color space using a color reference card (QPcard 203, QPcard AB, Sweden) and a quadratic correction model (Leon et al. 2006). Conversion from RGB to L*a*b* was performed in conjunction with a color correction using the color reference card because this method can accurately convert device-dependent RGB colors to device-independent L*a*b* colors (Leon et al. 2006).

Based on the results from previous work, L* and a* values were selected as the time-temperature indicators in the mashed potato model food (Bornhorst et al. 2017b) and a* value was selected as the time-temperature indicator in the green pea model food (Bornhorst et al. 2017c). L* value in the green pea model and b* value in both models were disregarded due to insignificant Pearson correlation coefficients between the color parameter and heating time (Bornhorst et al. 2017b, c).

For each sample layer, image analysis included cropping the image to minimize the background color, color correction, analysis of pixel values, and color mapping. In color mapping, L* values (mashed potato) and a* values (mashed potato and green pea) were converted to a jet color scale in MATLAB (Bornhorst et al. 2017b, c). Mashed potato color maps used an L* value range of 20–68 and a* value range of 1–22, as described by Bornhorst et al. (2017b). Green pea color maps used an a* value range of −22–1, as described by Bornhorst et al. (2017c). Color mapping helped visualize the heating pattern and color differences between samples. All four images from each tray of model food were assembled into a 3-D rendering using Adobe Photoshop (CS6 Version 13.0.1, Adobe Systems Incorporated, San Jose, CA, USA).

Statistical analysis (SAS® 9.2, SAS Institute Inc., Cary, NC, USA) was employed to develop normalized histograms using the total number of pixels in each image to normalize the pixel data. Descriptive statistics, including the median (50th percentile) and interquartile range were determined for each image. Interquartile range (IQR) of a sample's pixel data was calculated using the following:
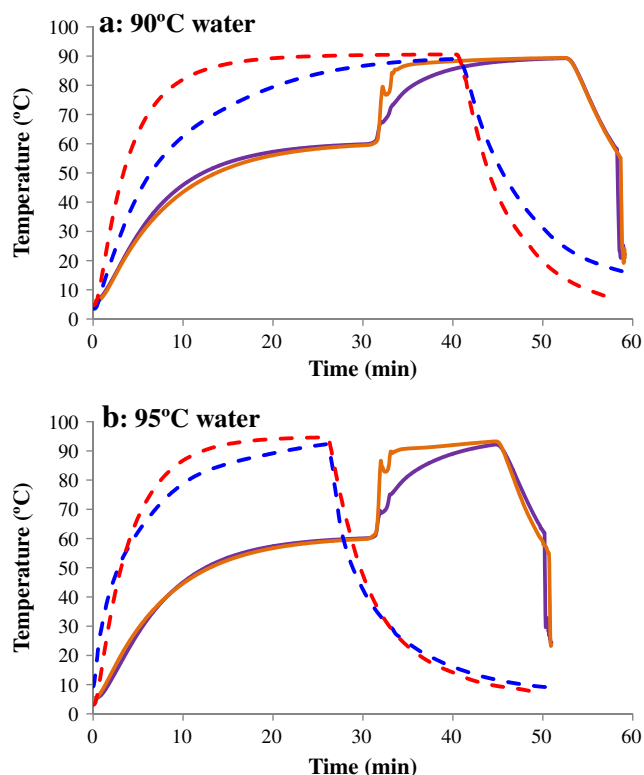
$$IQR = |Q_3 - Q_1| \qquad (3)$$

where Q_3 is the third quartile or 75th percentile and Q_1 is the first quartile or 25th percentile.

Results and Discussion

Thermal Process Severity

Typical temperature profiles at the cold and hot spots for each process are shown in Fig. 2. The model foods heated in the MAPS had a much shorter come-up time for the cold spot to reach the target temperature. For the mashed potato model food, the temperature at the cold spot increased from 60 to 89 °C in 9.8 min for the MAPS at 95 °C, 15.2 min for the hot

coldest spot of the model food product. The total process time in the hot water to produce a safely pasteurized food ranged between 10.3 and 40.2 min (Table 1). By increasing the water temperature 5 °C, the heating and holding time was reduced by 5.4–7.5 min for the MAPS processes and 14.2 min for the hot water processes. This time savings resulted in a decreased cook value at the cold and hot spots for the 95 °C processes, which implied the higher temperature, shorter time 95 °C processes should produce a better quality food.

For both model foods, the longest process (hot water 90 °C) resulted in the largest hot spot cook values of 11.3 min for mashed potato and 18.2 min for green pea. For both model foods, the shortest process (MAPS 95 °C) resulted in the smallest hot spot cook values of 6.5 min for mashed potato and 13.6 min for green pea. Based on the time-temperature data and cook value assessment, the model foods pasteurized in the hot water 90 °C process were expected to have the most color change and worst quality among the four processes. Conversely, the model foods pasteurized in the MAPS 95 °C process were expected to have the least color change and best quality among the four processes.

Fig. 2 Typical temperature profiles for 280-g trays of mashed potato model foods that achieved a minimum heat treatment equivalent of 90 °C for 10 min at the cold spot to control nonproteolytic *C. botulinum* spores. Processes used water temperatures of 90 °C (**a**) and 95 °C (**b**); cold and hot spot temperatures were measured for the microwave-assisted pasteurization system (MAPS) cold spot (——) and hot spot (——), and hot water process cold spot (— — —) and hot spot (— — —) (color figure online)

water method at 95 °C, 19.1 min for the MAPS at 90 °C, and 30.7 min for the hot water method at 90 °C.

As expected, the processes conducted in 90 °C water took a longer time than those in 95 °C water to adequately heat the

Color Change Assessment

Color change in mashed potato and green pea model foods was assessed in the top, middle, quarter, and bottom layers (Fig. 3). By organizing the images into 3-D renderings, it was possible to volumetrically visualize the color change and potential quality of the food. This visualization technique is a unique method and differed from the previous pasteurization validation studies with these model foods (Bornhorst et al. 2017b, c).

Table 1 Processing conditions for each model food to achieve a minimum accumulated thermal lethality (F_{90}) of 10 min at the cold spot to control nonproteolytic *C. botulinum* spores. Accumulated thermal lethality (F_{90}) and accumulated cook value (C_{100}) for the cold spots and hot spots were calculated for each process using z-values of 10 °C for F_{90} in both models and 23 °C for C_{100} in the mashed potato model food and 40 °C for C_{100} in the green pea model food

Model	Processing conditions			F_{90} (min)		C_{100} (min)	
	System	Preheating time and water temp.	Heating and holding time and water temp.	Cold spot	Hot spot	Cold spot	Hot spot
Mashed potato	MAPS	30 min 60 °C	17.8 min 90 °C	10.4	14.5	5.9	7.1
			10.3 min 95 °C	10.1	19.9	4.6	6.5
	Hot water	None	40.2 min 90 °C	10.4	27.8	6.4	11.3
			26.0 min 95 °C	12.2	35.1	5.4	9.1
Green pea	MAPS	30 min 60 °C	15.8 min 90 °C	10.3	24.2	12.2	14.6
			10.4 min 95 °C	12.8	39.4	10.8	13.6
	Hot water	None	40.2 min 90 °C	10.3	26.4	14.1	18.2
			26.0 min 95 °C	10.8	29.8	9.4	15.1
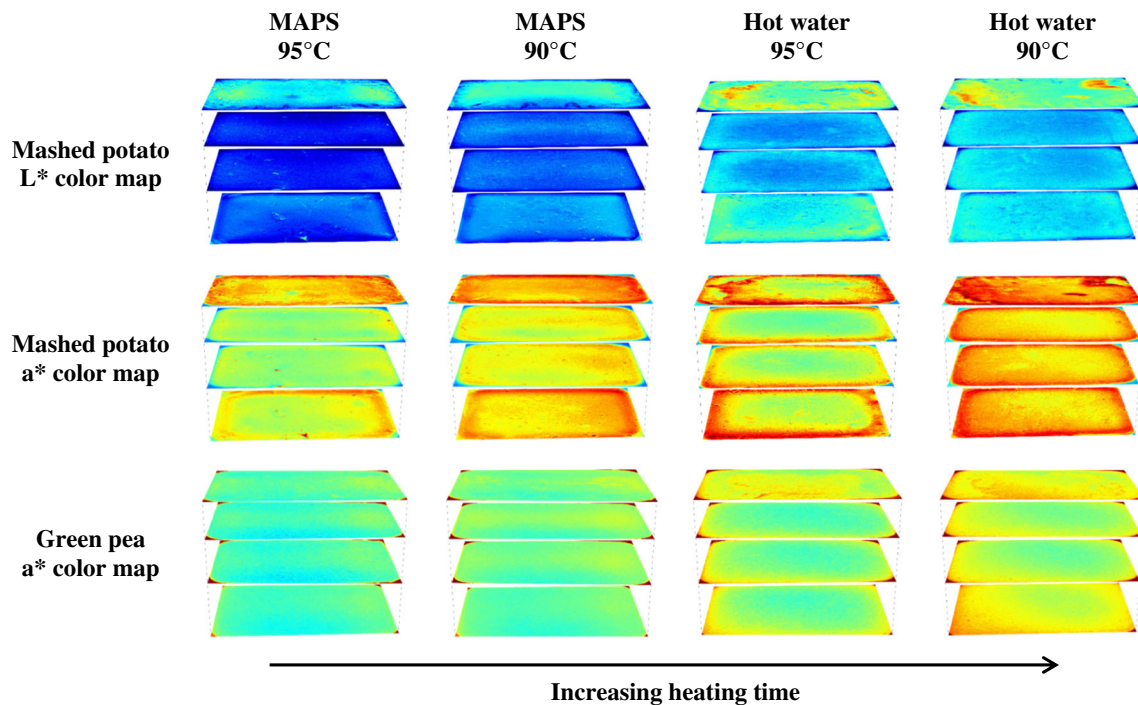
Fig. 3 Color change in mashed potato and green pea model foods pasteurized in the microwave-assisted pasteurization system (MAPS) and hot water processes with 90 and 95 °C water temperatures. Example images from a single tray of model food (top, middle, quarter, and bottom layers) were combined to create a 3-D rendering of the color change using L* and a* color mapping (color figure online)

The images (Fig. 3) showed that as hot water heating time increased, the amount of color change increased, which implied the food quality decreased; this was especially apparent when comparing the MAPS 95 °C and hot water 90 °C processes. From an overall visual inspection of all layers and models, the samples pasteurized with the MAPS 95 °C process had less color change than those from the hot water 90 °C process, which matched expectations based on the time-temperature data and cook value analysis.

Across all samples, the top layer had the most color change and the middle layer had the least color change. This matched expectations based on heat transfer theory and time-temperature data, as the outside of the package received a more severe heat treatment than the middle. The remaining analysis focused on these two extremes: the top layer that was the most heated with the greatest amount of color change and the middle layer that was the least heated with the smallest amount of color change. By examining both layers quantitatively, it was possible to capture both ends of the spectrum, the less heated areas and the overheated or burnt areas.

Normalized histograms of the L* values for the top and middle layers of the mashed potato model foods confirmed visual observations that the top layer had quantifiably more color change (smaller L* value) than the middle layer (Fig. 4). In the middle layer, the MAPS 95 °C process yielded the least color change from the control, with a median L* value of 68.8 ± 2.3, while the hot water 90 °C process had the greatest color change with a median L* value of 63.8 ± 1.4 (Table 2).

This level of color change should be detectable by consumers, as it's significantly larger than the threshold of human detection for color changes, which was found to be a total color difference (ΔE) between 0.1 and 2 (Huang et al. 1970a, b; Mahy et al. 1994). Top layer L* values had greater spread (Fig. 4a) with IQRs of 3.8–6.3 compared to the middle layer (2.4–3.6) and the unheated control (2.0). This implied that IQR was an indicator of uneven heating and burnt areas on the top surface of the model food trays. In the middle layer, all processes resulted in a similar IQR, which matched the findings of Bornhorst et al. (2017b, c), who concluded that IQR was similar for all middle layer samples.

Top and middle layer mashed potato model food a* values (Table 3) followed the same trends as L* values, with the models from the MAPS 95 °C process having the least color change (median a* value 11.7 ± 0.7) and the hot water 90 °C process had the most color change (median a* value 13.8 ± 0.9). Overall, the consumer would likely be able to see color differences between the mashed potato model food pasteurized in the MAPS 95 °C and hot water 90 °C based on both the L* and a* color differences.

Histograms of the a* value for the top and middle layer of the green pea model foods showed the MAPS 95 °C process having more pixels with less color change compared to the more severe hot water 90 °C process (Fig. 5). This trend was quantified using median values; the MAPS 95 °C process had less color change with median a* values of −12.2 ± 0.5 in the middle layer and −11.8 ± 0.5 in the top layer compared to the

a: Top layer
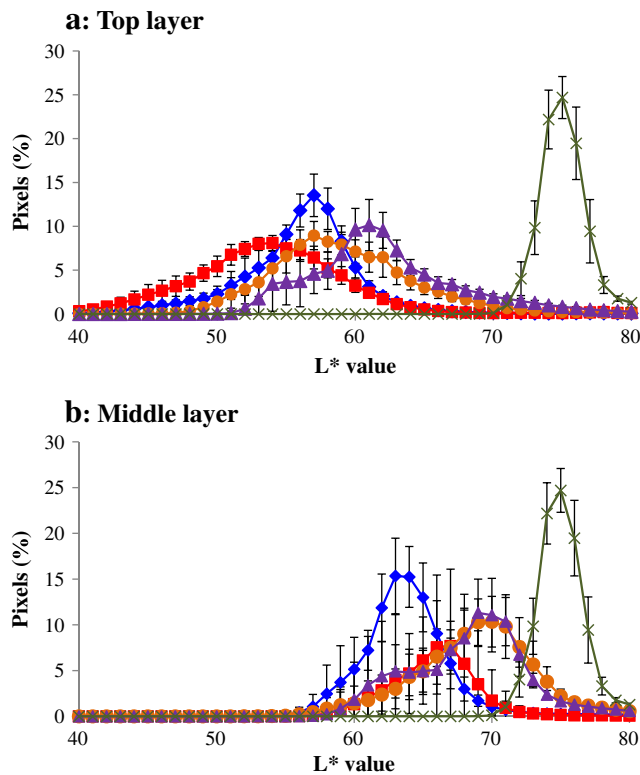
b: Middle layer

Fig. 4 Histograms of normalized, average L* value pixel data (eight replicates) for the top layer (**a**) and middle layer (**b**) of pasteurized mashed potato model food of the control (unheated) samples (×), microwave-assisted pasteurization system (MAPS) with 90 °C water (▲), MAPS with 95 °C water (●), hot water process with 90 °C water (◆), and hot water process with 95 °C water (■) (color figure online)

hot water 90 °C process with median color a* values of −9.9 ± 0.9 in the middle layer and −8.0 ± 0.6 in the top layer (Table 4). The spread of the a* value data from the middle and top layers were not significantly different, with middle layer IQRs ranging from −1.9 to −1.3 compared to the top layer with −1.8 to −1.2 and the unheated control of −1.5. This result indicated that there were fewer burnt areas in the green pea model compared to the mashed potato, which could be explained by the different temperature sensitivity of each model.
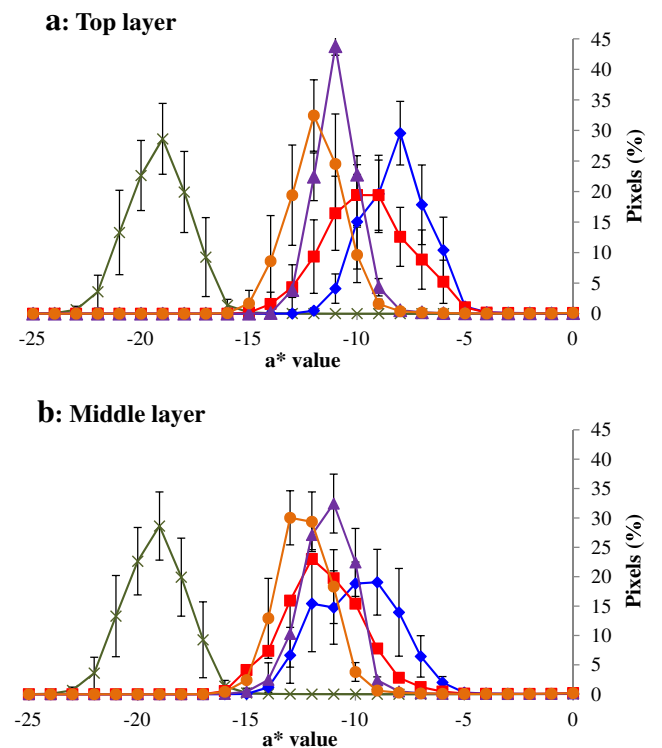
Table 2 Median and interquartile range (IQR) variations in L* value for the middle and top layers of mashed potato model food pasteurized in the microwave-assisted pasteurization system (MAPS) and hot water processes with 90 and 95 °C water temperatures compared to the unheated control

Processing conditions		Middle layer		Top layer	
		Median	IQR	Median	IQR
MAPS	95 °C	68.8 ± 2.3	3.6 ± 0.3	58.8 ± 1.7	5.6 ± 0.6
	90 °C	66.7 ± 2.2	3.3 ± 0.2	60.0 ± 1.9	6.0 ± 0.5
Hot water	95 °C	65.9 ± 1.5	2.7 ± 0.2	51.9 ± 0.8	6.3 ± 0.9
	90 °C	63.8 ± 1.4	2.4 ± 0.2	56.6 ± 1.2	3.8 ± 1.3
Control	Unheated	75.3 ± 0.6	2.0 ± 0.2	–	–

Table 3 Median and interquartile range (IQR) variations in a* value for the middle and top layers of mashed potato model food pasteurized in the microwave-assisted pasteurization system (MAPS) and hot water processes with 90 and 95 °C water temperatures compared to the unheated control

Processing conditions		Middle layer		Top layer	
		Median	IQR	Median	IQR
MAPS	95 °C	11.7 ± 0.7	1.2 ± 0.3	14.5 ± 0.9	1.8 ± 0.1
	90 °C	12.9 ± 0.8	1.4 ± 0.1	14.6 ± 1.1	2.0 ± 0.1
Hot water	95 °C	12.3 ± 0.7	2.5 ± 0.3	15.7 ± 0.7	3.1 ± 0.3
	90 °C	13.8 ± 0.9	2.0 ± 0.2	15.7 ± 0.8	2.8 ± 0.2
Control	Unheated	2.1 ± 0.4	1.3 ± 0.2	–	–

The color change (L* value) in the mashed potato model food was more sensitive to temperature changes with a reported z-value of 20.8 ± 6.9 °C (Bornhorst et al. 2017b) compared to the green pea model with a z-value of 39.9 ± 2.4 °C for a* value (Bornhorst et al. 2017c). Thus, the increased temperature sensitivity in the mashed potato model could explain the greater number of burnt areas and increased top layer IQR compared to the green pea model.

a: Top layer

b: Middle layer

Fig. 5 Histograms of normalized, average a* value pixel data (eight replicates) for the top layer (**a**) and middle layer (**b**) of pasteurized green pea model food of the control (unheated) samples (×), microwave-assisted pasteurization system (MAPS) with 90 °C water (▲), MAPS with 95 °C water (●), hot water process with 90 °C water (◆), and hot water process with 95 °C water (■) (color figure online)

Table 4 Median and interquartile range (IQR) variations in a* value for the middle and top layers of green pea model food pasteurized in the microwave-assisted pasteurization system (MAPS) and hot water processes with 90 and 95 °C water temperatures compared to the unheated control

Processing conditions		Middle layer		Top layer	
		Median	IQR	Median	IQR
MAPS	95 °C	−12.2 ± 0.5	−1.4 ± 0.1	−11.8 ± 0.5	−1.2 ± 0.1
	90 °C	−11.0 ± 0.5	−1.3 ± 0.1	−10.7 ± 0.2	−1.2 ± 0.1
Hot water	95 °C	−11.4 ± 0.8	−1.9 ± 0.1	−9.3 ± 0.9	−1.8 ± 0.3
	90 °C	−9.9 ± 0.9	−1.7 ± 0.2	−8.0 ± 0.6	−1.5 ± 0.3
Control	Unheated	−19.4 ± 1.0	−1.5 ± 0.1	–	–

Results showed that color could be used as a time-temperature indicator in both mashed potato and green pea model foods to simulate overall food quality degradation. By testing two unique model foods with different color change mechanisms, a larger range of temperature sensitivities were covered during the process quality assessment. The temperature sensitivities of the model foods included z-values from 20 to 40 °C (Bornhorst et al. 2017b, c); this range covered the temperature sensitivity of most quality attributes, which have z-values between 15 and 50 °C (Holdsworth 1997; Peng et al. 2015). This approach to process quality evaluation combined recently developed model foods with image analysis techniques in order to generate new tools for quality evaluation of novel thermal processing technologies. The promising results in this case study suggested that these new tools could help overcome challenges in microwave assisted thermal process optimization by providing a way to assess and visualize product quality, as well as validate computer simulations.

Conclusions

Four pasteurization processes were developed to control nonproteolytic *C. botulinum* spores using two water temperatures (90 and 95 °C) in a MAPS and conventional hot water heating method. Color change was visualized volumetrically in the top, middle, quarter, and bottom layers of mashed potato and green pea model food trays using an image analysis technique developed in this study to create 3-D renderings. Median color values were useful in assessing overall color change in middle and top layers. Interquartile range was a helpful indicator of burnt areas on the top surface of the model food, especially in the more temperature-sensitive mashed potato model food.

Among the four pasteurization processes analyzed in this study, the MAPS with 95 °C water was the best process because it had the shortest heating time, the smallest hot spot cook values, and the smallest amount of color change, implying a better quality. Conversely, the hot water process with 90 °C water was the worst because it had the longest heating time, the largest hot spot cook values, and the largest amount of color change, implying a worse or lower quality. This case study demonstrated the relevance of using model foods and image analysis in assessing the potential quality of pasteurization processes. During microwave-assisted thermal process optimization, these new tools could be utilized to assess and visualize product quality and validate computer simulations.

In the future, the model foods could also be used to assess the quality of less severe pasteurization processes, such as a 70 °C for 2 min process to control *L. monocytogenes*. Future work for the 90 °C for 10 min process goal could include an assessment of even shorter times with higher temperatures, e.g., 100 °C water. In order for these studies to be possible, the current MAPS design would need to be modified to include overpressure, which would enable water temperatures at or above the boiling point of water. Additionally, food companies could utilize these image analysis methods and model foods to optimize the quality of pilot-scale or industrial pasteurization processes.

References

Avila, I., Smout, C., Silva, C. L. M., & Hendrickx, M. (1999). Development of a novel methodology to validate optimal sterilization conditions for maximizing the texture quality of white beans in glass jars. *Biotechnology Progress, 15*(3), 565–572.

Benlloch-Tinoco, M., Igual, M., Salvador, A., Rodrigo, D., & Martínez-Navarrete, N. (2014). Quality and acceptability of microwave and conventionally pasteurised kiwifruit puree. *Food and Bioprocess Technology, 7*(11), 3282–3292.

Bornhorst, E. R., Tang, J., Sablani, S. S., & Barbosa-Cánovas, G. V. (2017a). Development of model food systems for thermal pasteurization applications based on Maillard reaction products. *LWT-Food Science and Technology, 75*, 417–424.

Bornhorst, E. R., Tang, J., Sablani, S. S., & Barbosa-Cánovas, G. V. (2017b). *Thermal pasteurization process evaluation using mashed potato model food with Maillard reaction products*. Under review: LWT-Food Science and Technology.

Bornhorst, E. R., Tang, J., Sablani, S. S., Barbosa-Cánovas, G. V., & Liu, F. (2017c). *Green pea and garlic puree model food development for thermal pasteurization process quality evaluation*. Under review: Journal of Food Science.

Chakraborty, S., Rao, P. S., & Mishra, H. N. (2015). Response surface optimization of process parameters and fuzzy analysis of sensory data of high pressure-temperature treated pineapple puree. *Journal of Food Science, 80*(8), E1763–E1775.

Chandrasekaran, S., Ramanathan, S., & Basak, T. (2013). Microwave food processing—a review. *Food Research International, 52*(1), 243–261.

Cha-um, W., Rattanadecho, P., & Pakdee, W. (2011). Experimental and numerical analysis of microwave heating of water and oil using a rectangular wave guide: influence of sample sizes, positions, and microwave power. *Food and Bioprocess Technology, 4*(4), 544–558.

Chen, H., Tang, J., & Liu, F. (2008). Simulation model for moving food packages in microwave heating processes using conformal FDTD method. *Journal of Food Engineering, 88*(3), 294–305.

Commonwealth Scientific and Industrial Research Organization (CSIRO). (2010). *Make it safe: A guide to food safety*. Collingwood: CSIRO Publishing.

Datta, A. K. (2008). Status of physics-based models in the design of food products, processes, and equipment. *Comprehensive Reviews in Food Science and Food Safety, 7*(1), 121–129.

Datta, A. K., & Anantheswaran, R. C. (2001). *Handbook of microwave technology for food applications (pp. 18–19)*. New York, NY: Marcel Dekker, Inc..

European Chilled Food Federation (ECFF). (2006). Recommendations for the production of prepackaged chilled food. 2nd ed. European Chilled Food Federation.

Food and Drug Administration (FDA). (2011). *Fish and fisheries products hazards and control guidance* (4nd ed.) U.S. Department of Health and Human Services.

Hildenbrand, P. (1980). An approach to solving the optimal temperature control problem for sterilization of conduction-heating foods. *Journal of Food Process Engingeering, 3*(3), 123–142.

Holdsworth, S. D. (1997). *Thermal processing of packaged foods (ch. 4 & 7)* (1st ed.). New York, NY: Blackie Academic & Professional.

Huang, I.-L., Francis, F. J., & Clydesdale, F. M. (1970a). Colorimetry of foods. 2. Color measurement of squash puree using the Kubelka-Munk concept. *Journal of Food Science, 35*(3), 315–317.

Huang, I.-L., Francis, F. J., & Clydesdale, F. M. (1970b). Colorimetry of foods. 3. Carrot puree. *Journal of Food Science, 35*(6), 771–773.

Leon, K., Mery, D., Pedreschi, F., & Leon, J. (2006). Color measurement in L*a*b* units from RGB digital images. *Food Research International, 39*(10), 1084–1091.

Lespinard, A. R., Arballo, J. R., Taus, F. J., & Mascheroni, R. H. (2015). Multi-objective optimization of the pasteurization process of pumpkin cubes packaged in glass jars. *International Journal of Food Engineering, 11*(5), 679–689.

Luan, D., Tang, J., Pedrow, P. D., Liu, F., & Tang, Z. (2013). Using mobile metallic temperature sensors in continuous microwave assisted sterilization (MATS) systems. *Journal of Food Engineering, 119*, 552–560.

Mahy, M., Van Eyckden, L., & Ooosterlinkc, A. (1994). Evaluation of the uniform color spaces developed after the adoption of CIELAB and CIELUV. *Color Research Application, 19*(2), 105–121.

Marszalek, K., Wozniak, L., Skapska, S., & Mitek, M. (2016). A comparative study of the quality of strawberry purée preserved by continuous microwave heating and convetional thermal pasteurization during long-term cold storage. *Food and Bioprocess Technology, 9*(7), 1100–1112.

Miri, T., Tsoukalas, A., Bakalis, S., Pistikopoulos, E. N., Rustem, B., & Fryer, P. J. (2008). Global optimization of process conditions in batch thermal sterilization of food. *Journal of Food Engingeering, 87*(4), 485–494.

Pathak, S. K., Liu, F., & Tang, J. (2003). Finite domain time domain (FDTD) characterization of a single model applicator. *Journal of Microwave Power and Electromagnetic Energy, 38*(1), 37–48.

Peck, M. W. (2006). Clostridium botulinum and the safety of minimally heated, chilled foods: An emerging issue? *Journal of Applied Microbiolgy, 101*(3), 556–570.

Peng, J., Tang, J., Barrett, D. M., Sablani, S. S., Anderson, N., & Powers, J. R. (2015). Thermal pasteurization of vegetables: critical factors for process design and effects on quality. *Critical Reviews in Food Science and Nutrition*, 00–00.

Renna, M., Pace, B., Cefola, M., Santamaria, P., Serio, F., & Gonnella, M. (2013). Comparison of two jam making methods to preserve the quality of colored carrots. *LWT-Food Science and Technology, 53*(2), 547–554.

Resurreccion Jr., F. P., Tang, J., Pedrow, P., Cavalieri, R., Liu, F., & Tang, Z. (2013). Development of a computer simulation model for processing food in a microwave assisted thermal sterilization (MATS) system. *Journal of Food Engineering, 118*(4), 406–416.

Singh, A. P., & Ramaswamy, H. S. (2015). Effect of can orientation on heat transfer coefficients associated with liquid particulate mixtures during reciprocation agitation thermal processing. *Food and Bioprocess Technology, 8*(7), 1405–1418.

Smout, C., Banadda, N. E., Van Loey, A. M. L., & Hendrickx, M. E. G. (2003). Nonuniformity in lethality and quality in thermal process optimization: a case study on color degradation of green peas. *Journal of Food Science, 68*(2), 545–550.

Tang, J. (2015). Unlocking potentials of microwaves for food safety and quality. *Journal of Food Science, 80*(8), E1776–E1793.

Teixeira, A. A., Dixon, J. R., Zahradnik, J. W., & Zinsmeister, G. E. (1969). Computer optimization of nutrient retention in the thermal processing of conduction-heated foods. *Food Technology, 23*, 845–850.

Teixeira, A. A., Stumbo, C. R., & Zahradnik, J. W. (1975). Experimental evaluation of mathematical and computer models for thermal process evaluation. *Journal of Food Science, 40*(4), 653–655.